MICROWAVE LABORATORY REPORT NO. 88-P-5

THE BOUNDARY-INTEGRAL METHOD FOR PLANAR MICROSTRIP CIRCUITS

TECHNICAL REPORT

SANCHI SANDY CHANG AND TATSUO ITOH

DECEMBER 1988

ARMY RESEARCH OFFICE

CONTRACT DAAL03-88-K-0005

THE UNIVERSITY OF TEXAS

DEPARTMENT OF ELECTRICAL ENGINEERING

AUSTIN, TEXAS 78712

UNCLASSIFIED
SECURITY CLASSIFICATION OF THIS PAGE

MASTER COPY - FOR REPRODUCTION PURPOSES

REPORT DOCUMENTATION PAGE

1a. REPORT SECURITY CLASSIFICATION: Unclassified	1b. RESTRICTIVE MARKINGS
2a. SECURITY CLASSIFICATION AUTHORITY	3. DISTRIBUTION/AVAILABILITY OF REPORT: Approved for public release; distribution unlimited.
2b. DECLASSIFICATION/DOWNGRADING SCHEDULE	
4. PERFORMING ORGANIZATION REPORT NUMBER(S): Microwave Laboratory Report No. 88-P-5	5. MONITORING ORGANIZATION REPORT NUMBER(S): ARO 25045.11-EL
6a. NAME OF PERFORMING ORGANIZATION: The University of Texas; 6b. OFFICE SYMBOL (If applicable)	7a. NAME OF MONITORING ORGANIZATION: U. S. Army Research Office
6c. ADDRESS (City, State, and ZIP Code): Dept. of Electrical & Computer Engineering, Austin, Texas 78712	7b. ADDRESS (City, State, and ZIP Code): P. O. Box 12211, Research Triangle Park, NC 27709-2211
8a. NAME OF FUNDING/SPONSORING ORGANIZATION: U. S. Army Research Office; 8b. OFFICE SYMBOL (If applicable)	9. PROCUREMENT INSTRUMENT IDENTIFICATION NUMBER: DAAL03-88-K-0005
8c. ADDRESS (City, State, and ZIP Code): P. O. Box 12211, Research Triangle Park, NC 27709-2211	10. SOURCE OF FUNDING NUMBERS: PROGRAM ELEMENT NO. / PROJECT NO. / TASK NO. / WORK UNIT ACCESSION NO

11. TITLE (Include Security Classification): The Boundary-Integral Method for Planar Microstrip Circuits

12. PERSONAL AUTHOR(S): Sanchi Sandy Chang and Tatsuo Itoh

13a. TYPE OF REPORT	13b. TIME COVERED	14. DATE OF REPORT (Year, Month, Day)	15. PAGE COUNT
Technical	FROM _____ TO _____	Dec. 1988	38

16. SUPPLEMENTARY NOTATION: The view, opinions and/or findings contained in this report are those of the author(s) and should not be construed as an official Department of the Army position, policy, or decision, unless so designated by other documentation.

17 COSATI CODES		
FIELD	GROUP	SUB-GROUP

18. SUBJECT TERMS (Continue on reverse if necessary and identify by block number): Boundary-integral method, T-junction, Right Angle Bend, Planar Microstrip Circuit

19. ABSTRACT (Continue on reverse if necessary and identify by block number)

The main subject of this thesis is to develop a general purpose computer program for the analysis containing a planar microstrip circuit arbitrarily shaped. Based on the boundary-integral method (also called the contour-integral method), the analyses of circuits containing right-angled microstrip bend with or without a miter cut and circuits of a T-junctions with or without a V-shaped cut are presented in this thesis. Scattering parameters and other related data of the circuits are calcualted and presented. They agree well with published data. It is shown that the boundary-integral method is an applicable and effective computer-aided design tool for microstrip circuits of more complicated geometries.

20. DISTRIBUTION/AVAILABILITY OF ABSTRACT: ☐ UNCLASSIFIED/UNLIMITED ☐ SAME AS RPT. ☐ DTIC USERS	21. ABSTRACT SECURITY CLASSIFICATION: Unclassified
22a NAME OF RESPONSIBLE INDIVIDUAL	22b TELEPHONE (Include Area Code) / 22c OFFICE SYMBOL

DD FORM 1473, 84 MAR — 83 APR edition may be used until exhausted. All other editions are obsolete.

SECURITY CLASSIFICATION OF THIS PAGE
UNCLASSIFIED

MICROWAVE LABORATORY REPORT NO. 88-P-5

THE BOUNDARY-INTEGRAL METHOD FOR PLANAR MICROSTRIP CIRCUITS

TECHNICAL REPORT

SANCHI SANDY CHANG AND TATSUO ITOH

DECEMBER 1988

ARMY RESEARCH OFFICE

CONTRACT DAAL03-88-K-0005

THE UNIVERSITY OF TEXAS

DEPARTMENT OF ELECTRICAL ENGINEERING

AUSTIN, TEXAS 78712

Abstract

THE BOUNDARY-INTEGRAL METHOD

FOR PLANAR MICROSTRIP CIRCUITS

The main subject of this thesis is to develop a general purpose computer program for the analysis containing a planar microstrip circuit arbitrarily shaped. Based on the boundary-integral method (also called the contour-integral method), the analyses of circuits containing right - angled microstrip bend with or without a miter cut and circuits of a T-junctions with or without a V-shaped cut are presented in this thesis. Scattering parameters and other related data of the circuits are calculated and presented. They agree well with published data. It is shown that the boundary-integral method is an applicable and effective computer-aided design tool for microstrip circuits of more complicated geometries.

Table of Contents

List of Figures

Introduction

In the development of microwave integrated circuits (MIC) and millimeter-wave integrated circuits (MMIC), the planar microstrip line technique gained much attention mainly due to the fact that the mode of propagation on the microstrip line is almost TEM. The so called waveguide model has been applied successfully to a number of microstrip discontinuities. Microstrip circuits are often accompanied by discontinuities of one type or another, of which, the most common forms are the right-angled bend and T-junction. The geometries of the circuits analyzed are shown in Figures 1 and Figures 2. In order to simplify the analysis and to make use of well developed waveguide techniques, the microstrip line circuits are usually replaced by equivalent parallel-plate waveguides with magnetic side walls (as shown in Fig.3). After each microstrip line network is replaced with a closed structure, the microstrip discontinuity problem becomes that of a closed waveguide. Due to the discrete nature of modal spectrum in closed structure, the analysis of the scattering from the discontinuity is handled rather easily, typically by a mode - matching method.

There are many methods that can be used to analyze planar circuits, such as eigenvalue method, or the Rayligh-Ritz method. For planar circuits with simple geometrical shapes, like circles or rectangles shapes, the eigenvalue method can be readily used.

The Rayleigh-Ritz method or finite element method on the other hand can be used to solve more complicated planar circuits. However, the computation of eigenfunctions over the entire area of the circuit pattern is time-consuming. The segmentation and desegmentation methods [1][2] can be used to analyze irregular complicated circuits, but there are some limitations on the shapes of such circuits. Details of these methods of analysis as well as their limitations were discussed in more detail in a number of articles [1],[2],[3],[4].

For an arbitrarily shaped planar circuit, using the boundary-integral equation method to develop a general purpose computer program to do the analysis is effective, accurate and adaptable since only the voltage and the current along the periphery of the circuit -- not the entire area of the circuit -- need to be considered. Circuit parameters can be derived from the boundary-integral equation method directly. Hence, analysis of more complicated circuits can be handled easily and the computer time is reduced.

In the next section, this boundary-integral equation method is discribed. The process of program design is also given. In the subsequent section, results based on the formulation are presented in terms of the scattering parameters, and a comparison of results obtained by different numbers of sampling points along the periphery is also presented.

Formulation

Based on the two-dimensional planar circuit presented and introduced in [5], a planar microstrip model with an arbitrary shape is considered. It is filled with material of effective permittivity ε_{re} and the effective width is W_{eff}. There are several coupling ports located around the planar circuits. We divide the circuit periphery into N incremental sections numbered as 1,2,3,.....,N, having width $W_1, W_2, W_3, \ldots, W_n$, respectively. Coupling ports are assumed to occupy two or more sections (as illustrated in Fig.4). Sampling points are set at the center of each section, and the magnetic and electric field intensities are assumed to be constant over each section.

Using Weber's solution for cylindrical waves[6], the potential at each sampling point along the periphery is satisfied by the following matrix equations :

$$\sum_{j=1}^{N} u_{ij} V_j = \sum_{j=1}^{N} h_{ij} I_j \qquad (1)$$

$$u_{ij} = 1 \qquad (i = j)$$

$$= \delta_{ij} - \frac{k}{2j} \int_{w_j} \cos\theta_{ij} H_1^{(2)}(kr)\, ds \qquad (2)$$

$$h_{ij} = \frac{\omega\mu d}{4} \frac{1}{W_j} \int_{w_j} H_0^{(2)}(kr)\, ds$$

$$= \frac{\omega\mu d}{4} \left[1 - \frac{2j}{\pi} \left(\ln \frac{k w_j}{4} - 1 + \gamma \right) \right] \qquad (i = j) \qquad (3)$$

$\gamma = 0.5772.....$ (Euler's constant) $\quad k=\omega\sqrt{\varepsilon_r \varepsilon_0 \mu_0}$

where $I_j = -2i_h W_j$: the total current flowing into the jth port on both the upper and lower surfaces of the circuit plates.

$H_0^{(2)}$, $H_1^{(2)}$: the zeroth order and the first order Hankel function of the second kind, respectinely.

d : the thickness of dielectric layer .

r_{ij} and θ_{ij} : the distance between the ith and jth coupling ports and the angle made by the line connecting these points and the normal at the jth sampling point .

The rf voltage of each sampling point can be obtained by solving (1):

$$\begin{pmatrix} 1 & \cdots & U_{1n} \\ U_{21} & 1 & \cdots & U_{2n} \\ \cdots & \cdots & \cdots & \cdots \\ \cdots & & 1 & U_{(n-1)n} \\ \cdots & \cdots & \cdots & 1 \\ U_{n1} & \cdots & \cdots & \end{pmatrix} \begin{pmatrix} V_1 \\ V_2 \\ \vdots \\ \vdots \\ V_n \end{pmatrix} = \begin{pmatrix} h_{11} & \cdots & \cdots & h_{1n} \\ h_{21} & \cdots & \cdots & h_{2n} \\ \cdots & \cdots & \cdots & \cdots \\ \cdots & \cdots & \cdots & \cdots \\ h_{n1} & \cdots & \cdots & h_{nn} \end{pmatrix} \begin{pmatrix} I_1 \\ I_2 \\ \vdots \\ \vdots \\ I_n \end{pmatrix}$$

$$[V] = \mathbf{U}^{-1}\mathbf{H}\,[I] \tag{4}$$

$$[V] = [\mathbf{Z}]_{\mathbf{hxn}}\,[I] \tag{5}$$

$$\begin{pmatrix} V_1 \\ V_2 \\ \vdots \\ V_n \end{pmatrix} = \begin{pmatrix} Z_{11} & \cdots & Z_{1n} \\ Z_{21} & \cdots & Z_{2n} \\ \cdots & \cdots & \cdots \\ \cdots & \cdots & \cdots \\ Z_{n1} & \cdots & Z_{nn} \end{pmatrix} \begin{pmatrix} I_1 \\ I_2 \\ \vdots \\ I_n \end{pmatrix} \tag{6}$$

$$[Z]_{nxn} = U^{-1} H \tag{7}$$

[Z] is an nxn matrix. It is considered that all n sections are coupling ports. In fact, most of the n ports described above are open circuits; in other words, most of the nxn elements of $[Z]_{nxn}$ are zero. Therefore$[Z]_{nxn}$, can be reduced by choosing only the necessary elements given by (7). The reduced matrix $[Z]_{NxN}$ is described in (8). N is the sum of all sampling points along all A ports. (As shown in Fig.5)

$$N=\sum_{i=1}^{A} m_i$$

m_i : the number of sampling points of ith port

$$[V]=[Z]_{NxN}[I] \tag{8}$$

$$
\begin{matrix} m_1 \\ m_2 \\ \vdots \\ m_A \end{matrix}
\begin{Bmatrix}
V_1^{(1)} \\ \vdots \\ V_{m1}^{(1)} \\
V_1^{(2)} \\ \vdots \\ V_{m2}^{(2)} \\
\vdots \\
V_1^{(A)} \\ \vdots \\ V_{mA}^{(A)}
\end{Bmatrix}
=
[Z]_{NxN}
\begin{Bmatrix}
I_1^{(1)} \\ \vdots \\ I_{m1}^{(1)} \\
I_1^{(2)} \\ \vdots \\ I_{m1}^{(2)} \\
\vdots \\
I_1^{(A)} \\ \vdots \\ I_{mA}^{(A)}
\end{Bmatrix}
\begin{matrix} \\ \\ m_1 \\ \\ \\ m_2 \\ \\ \\ m_A \end{matrix}
$$

$$
[Z]_{N\times N} =
\begin{bmatrix}
Z_{(p+1)(p+1)} \cdots Z_{(p+1)(p+m_1)} & Z_{(p+1)(q+1)} \cdots Z_{(p+1)(q+m_2)} & \cdots & Z_{(p+1)(r+1)} \cdots Z_{(p+1)(r+m_A)} \\
\vdots & \vdots & & \vdots \\
Z_{(p+m_1)(p+1)} \cdots Z_{(p+m_1)(p+m_1)} & Z_{(p+m_1)(q+1)} \cdots Z_{(p+m_1)(q+m_2)} & \cdots & Z_{(p+m_1)(r+1)} \cdots Z_{(p+m_1)(r+m_A)} \\
Z_{(q+1)(p+1)} \cdots Z_{(q+1)(p+m_1)} & Z_{(q+1)(q+1)} \cdots Z_{(q+1)(q+m_2)} & \cdots & Z_{(q+1)(r+1)} \cdots Z_{(q+1)(r+m_A)} \\
\vdots & \vdots & & \vdots \\
Z_{(q+m_2)(p+1)} \cdots Z_{(q+m_2)(p+m_1)} & Z_{(q+m_2)(q+1)} \cdots Z_{(q+m_2)(q+m_2)} & \cdots & Z_{(q+m_2)(r+1)} \cdots Z_{(q+m_2)(r+m_A)} \\
\vdots & \vdots & & \vdots \\
Z_{(r+1)(p+1)} \cdots Z_{(r+1)(p+m_1)} & Z_{(r+1)(q+1)} \cdots Z_{(r+1)(q+m_2)} & \cdots & Z_{(r+1)(r+1)} \cdots Z_{(r+1)(r+m_A)} \\
\vdots & \vdots & & \vdots \\
Z_{(r+m_A)(p+1)} \cdots Z_{(r+m_A)(p+m_1)} & Z_{(r+m_A)(q+1)} \cdots Z_{(r+m_A)(q+m_2)} & \cdots & Z_{(r+m_A)(r+1)} \cdots Z_{(r+m_A)(r+m_A)}
\end{bmatrix}
$$

(9)

The next step is to consider the higher order modes of each port by expanding the RF voltage and current density of each port in terms of m stripline modes.

$$V(X_K^{(i)}) = \sum_{L=1}^{m_i} \upsilon_L^{(i)} \cos\left[(L-1)\frac{X_K^{(i)}\pi}{W_i}\right] \tag{10}$$

$$I(X_K^{(i)}) = \sum_{L=1}^{m_i} \frac{1}{m_i} \upsilon_L^{(i)} \cos\left[(L-1)\frac{X_K^{(i)}\pi}{W_i}\right] \tag{11}$$

$X_K^{(i)}$: kth sampling point at the ith port

$k = 1,2,.....,m_i \qquad i = 1,2,.....,A$

υ_L : magnitude of modal voltageat each sampling point

m_i : the total number of sampling points at the ith port

$(i = 1,2,.....,A)$

W_i : width of the ith port

From Fig.5, we obtain the point

$$X_K^{(i)} = \frac{w_i}{2m_i} + \frac{w_i(k-1)}{m_i} = \frac{w_i(2k-1)}{2m_i}$$

So, equations (10) and (11) can be witten as follows:

$$V(X_K^{(i)}) = \sum_{L=1}^{m_i} \upsilon_L^{(i)} \cos\left[\frac{(L-1)\,\pi(2k-1)}{2m_i} \right] \qquad (12)$$

$$I(X_K^{(i)}) = \sum_{L=1}^{m_i} \frac{1}{m_i} \upsilon_L^{(i)} \cos\left[\frac{(L-1)\,\pi(2k-1)}{2m_i} \right] \qquad (13)$$

and then

$$V(X_1^{(1)}) = \upsilon_1^{(1)} + \upsilon_2^{(1)} \cos\left(\frac{\pi}{2m_1}\right) + \ldots\ldots\ldots\ldots\ldots\ldots\ldots\ldots + \upsilon_{m_1}^{(1)} \cos\left(\frac{(m_1-1)\pi}{2m_1}\right)$$

$$V(X_k^{(1)}) = \upsilon_1^{(1)} + \upsilon_2^{(1)} \cos\left(\frac{(2k-1)\pi}{2m_1}\right) + \ldots\ldots\ldots\ldots\ldots\ldots\ldots + \upsilon_{m_1}^{(1)} \cos\left(\frac{(2k-1)(m_1-1)\pi}{2m_1}\right)$$

$$V(X_{m_1}^{(1)}) = \upsilon_1^{(1)} + \upsilon_2^{(1)} \cos\left(\frac{(2m_1-1)\pi}{2m_1}\right) + \ldots\ldots\ldots\ldots\ldots + \upsilon_{m_1}^{(1)} \cos\left(\frac{(2m_1-1)(m_1-1)\pi}{2m_1}\right)$$

.

.

$$V(X_1^{(A)}) = \upsilon_1^{(A)} + \upsilon_2^{(A)} \cos\left(\frac{\pi}{2m_A}\right) + \ldots\ldots\ldots\ldots\ldots\ldots\ldots\ldots + \upsilon_{m_A}^{(A)} \cos\left(\frac{(m_A-1)\pi}{2m_A}\right)$$

$$V(X_k^{(A)}) = \upsilon_1^{(A)} + \upsilon_2^{(A)} \cos\left(\frac{(2k-1)\pi}{2m_A}\right) + \ldots\ldots\ldots\ldots\ldots\ldots + \upsilon_{m_A}^{(A)} \cos\left(\frac{(2k-1)(m_A-1)\pi}{2m_A}\right)$$

$$V(X_{m_A}^{(A)})=\upsilon_1^{(A)}+\upsilon_2^{(A)}\cos\left(\frac{(2m_A-1)\pi}{2m_A}\right)+\ldots\ldots\ldots\ldots+\upsilon_{m_A}^{(A)}\cos\left(\frac{(2m_A-1)(m_A-1)\pi}{2m_A}\right)$$

(14)

$$I(X_1^{(1)})=\frac{1}{m_1}\left(i_1^{(1)}+i_2^{(1)}\cos\left(\frac{\pi}{2m_1}\right)+\ldots\ldots\ldots\ldots\ldots\ldots i_{m_1}^{(1)}\cos\left(\frac{(m_1-1)\pi}{2m_1}\right)\right)$$

$$I(X_k^{(1)})=\frac{1}{m_1}\left(i_1^{(1)}+i_2^{(1)}\cos\left(\frac{(2k-1)\pi}{2m_1}\right)+\ldots\ldots\ldots\ldots\ldots+i_{m_1}^{(1)}\cos\left(\frac{(2k-1)(m_1-1)\pi}{2m_1}\right)\right)$$

$$I(X_{m_1}^{(1)})=i_1^{(1)}+i_2^{(1)}\cos\left(\frac{(2m_1-1)\pi}{2m_1}\right)+\ldots\ldots\ldots\ldots\ldots+i_{m_1}^{(1)}\cos\left(\frac{(2m_1-1)(m_1-1)\pi}{2m_1}\right)$$

.

.

$$I(X_1^{(A)})=\frac{1}{m_A}\left(i_1^{(A)}+i_{(A),2}\cos\left(\frac{\pi}{2m_A}\right)+\ldots\ldots\ldots\ldots\ldots\ldots+i_{m_A}^{(A)}\cos\left(\frac{(m_A-1)\pi}{2m_A}\right)\right)$$

$$I(X_k^{(A)})=\frac{1}{m_A}\left(i_1^{(A)}+i_2^{(A)}\cos\left(\frac{(2k-1)\pi}{2m_A}\right)+\ldots\ldots\ldots\ldots\ldots+i_{m_A}^{(A)}\cos\left(\frac{(2k-1)(m_A-1)\pi}{2m_A}\right)\right)$$

$$I(X_{m_A}^{(A)})=\frac{1}{m_A}\left(i_1^{(A)}+i_2^{(A)}\cos\left(\frac{(2m_A-1)\pi}{2m_A}\right)+\ldots\ldots\ldots+i_{m_A}^{(A)}\cos\left(\frac{(2m_A-1)(m_A-1)\pi}{2m_A}\right)\right)$$

(15)

$$\begin{pmatrix} V(X_1)^{(1)} \\ \vdots \\ V(X_{m1})^{(1)} \\ V(X_1)^{(2)} \\ \vdots \\ V(X_{m2})^{(2)} \\ \vdots \\ V(X_1)^{(A)} \\ \vdots \\ V(X_{mA})^{(A)} \end{pmatrix} = \begin{pmatrix} A^{(1)} & \cdots & 0 \\ \vdots & A^{(2)} & \vdots \\ & \ddots & \\ 0 & \cdots & A^{(A)} \end{pmatrix} \begin{pmatrix} \upsilon_{(x_1)}^{(1)} \\ \vdots \\ \upsilon_{(x_{m1})}^{(1)} \\ \upsilon_{(x_1)}^{(2)} \\ \vdots \\ \upsilon_{(x_{m2})}^{(2)} \\ \vdots \\ \upsilon_{(x_1)}^{(A)} \\ \vdots \\ \upsilon_{(x_{mA})}^{(A)} \end{pmatrix}$$

(Nx1) (NxN) (Nx1)

(16)

$$\begin{pmatrix} V(X)_{1}^{(1)} \\ \vdots \\ V(X)_{m1}^{(1)} \\ V(X)_{1}^{(2)} \\ \vdots \\ V(X)_{m2}^{(2)} \\ \vdots \\ V(X)_{1}^{(A)} \\ \vdots \\ V(X)_{mA}^{(A)} \end{pmatrix} = \begin{pmatrix} A^{(1)} & \cdots & 0 \\ \vdots & A^{(2)} & \vdots \\ 0 & \cdots & A^{(A)} \end{pmatrix} \begin{pmatrix} M^{(1)} & \cdots & 0 \\ \vdots & M^{(2)} & \vdots \\ 0 & \cdots & M^{(A)} \end{pmatrix} \begin{pmatrix} \upsilon(x_1)^{(1)} \\ \vdots \\ \upsilon(x_{m1})^{(1)} \\ \upsilon(x_1)^{(2)} \\ \vdots \\ \upsilon(x_{m2})^{(2)} \\ \vdots \\ \upsilon(x_1)^{(A)} \\ \vdots \\ \upsilon(x_{mA})^{(A)} \end{pmatrix} \quad (17)$$

(Nx1) (NxN) (NxN) (Nx1)

$$A^{(1)} = \begin{pmatrix} 1 & \cos\left(\frac{\pi}{2m_1}\right) & \cdots & \cos\left((m_1-1)\frac{\pi}{2m_1}\right) \\ 1 & \cos\left(\frac{3\pi}{2m_1}\right) & \cdots & \cos\left(3(m_1-1)\frac{\pi}{2m_1}\right) \\ \vdots & \vdots & & \vdots \\ 1 & \cos\left((2m_1-1)\frac{\pi}{2m_1}\right) & \cdots & \cos\left((2m_1-1)(m_1-1)\frac{\pi}{2m_1}\right) \end{pmatrix}$$

$$A^{(i)} = \begin{pmatrix} 1 & \cos\left(\frac{\pi}{2m_i}\right) & \cdots & \cos\left((m_i-1)\frac{\pi}{2m_i}\right) \\ 1 & \cos\left(\frac{3\pi}{2m_i}\right) & \cdots & \cos\left(3(m_i-1)\frac{\pi}{2m_i}\right) \\ \vdots & \vdots & & \vdots \\ 1 & \cos\left((2m_i-1)\frac{\pi}{2m_i}\right) & \cdots & \cos\left((2m_i-1)(m_i-1)\frac{\pi}{2m_i}\right) \end{pmatrix} \qquad (18)$$

$$A^{(A)} = \begin{pmatrix} 1 & \cos\left(\frac{\pi}{2m_A}\right) & \cdots & \cos\left((m_A-1)\frac{\pi}{2m_A}\right) \\ 1 & \cos\left(\frac{3\pi}{2m_A}\right) & \cdots & \cos\left(3(m_A-1)\frac{\pi}{2m_A}\right) \\ \vdots & \vdots & & \vdots \\ 1 & \cos\left((2m_A-1)\frac{\pi}{2m_A}\right) & \cdots & \cos\left((2m_A-1)(m_A-1)\frac{\pi}{2m_A}\right) \end{pmatrix}$$

$$M^{(1)} = \begin{pmatrix} \frac{1}{m_1} & \cdots & \frac{1}{m_1} \\ \vdots & & \vdots \\ \frac{1}{m_1} & \cdots & \frac{1}{m_1} \end{pmatrix}$$

$m_1 \times m_1$

$$M^{(2)} = \begin{bmatrix} \frac{1}{m_2} & \cdots & \frac{1}{m_2} \\ \vdots & & \vdots \\ \frac{1}{m_2} & \cdots & \frac{1}{m_2} \end{bmatrix}_{m_2 \times m_2} \tag{19}$$

$$M^{(A)} = \begin{bmatrix} \frac{1}{m_A} & \cdots & \frac{1}{m_A} \\ \vdots & & \vdots \\ \frac{1}{m_A} & \cdots & \frac{1}{m_A} \end{bmatrix}_{m_A \times m_A}$$

$$[V] = [Z]_{NxN}[I] \tag{20}$$

$$[A][\upsilon] = [Z][A][M][i] \tag{21}$$

$[\upsilon]$ and $[i]$ are Nx1 matrices

$[Z]$, $[A]$ and $[M]$ are NxN matrices

We define $[B] = [Z][A][M]$

$$[A][\upsilon] = [B][i] \tag{22}$$

For the purpose of separating the first order mode from higher order modes, the matrices [A], [B] are rearranged as below:

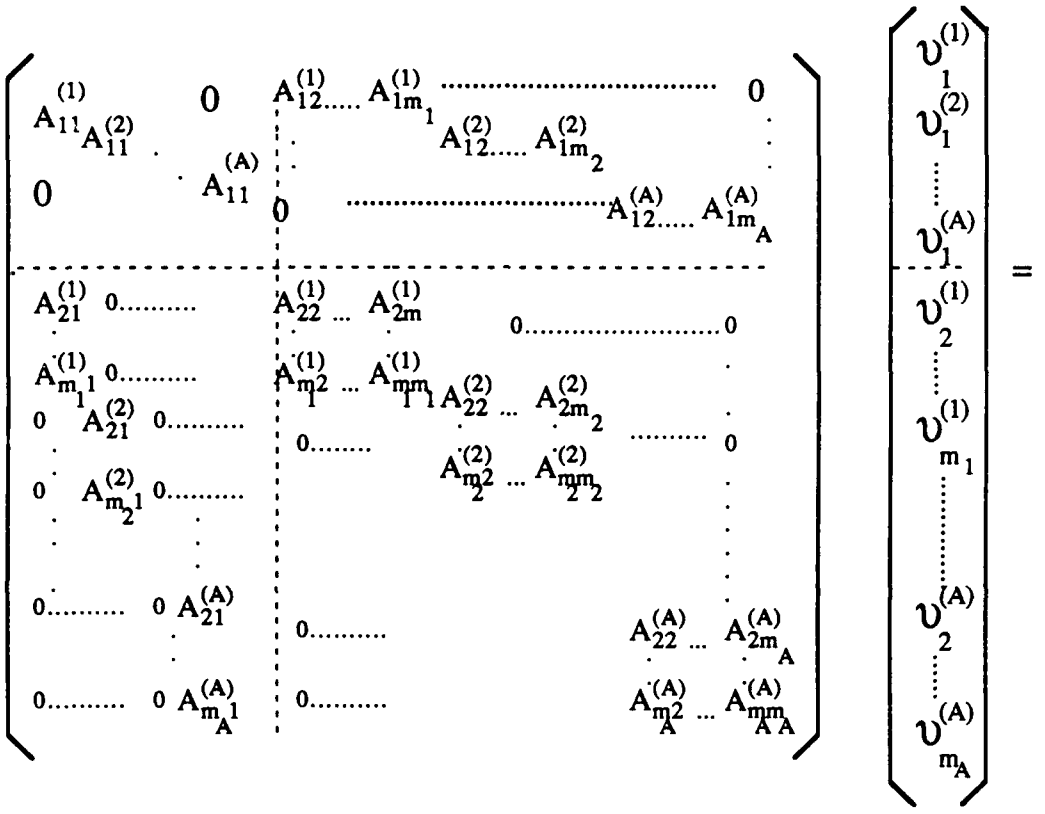

$$\begin{pmatrix} B_{11} & \cdots & B_{1,N-m_A+1} & B_{12} & \cdots & B_{1,N-m_A+2} & \cdots & B_{1N} \\ \vdots & & \vdots & \vdots & & & & \vdots \\ B_{N-m_A+1,1} & \cdots & B_{N-m_A+1,N-m_A+1} & B_{N-m_A+1,2} & \cdots & & & B_{N-m_A+1,N} \\ B_{21} & B_{2,m_1+1} \cdots & B_{2,N-m_A+1} & B_{22} & \cdots B_{2m_1} \cdots & & B_{2,N-m_A+2} \cdots & B_{2N} \\ \vdots & & \vdots & \vdots & & & & \\ B_{m_1 1} & & B_{m_1,N-m_A+1} & B_{m_1 2} \cdots & B_{m_1 m_1} \cdots & & & \\ \vdots & & \vdots & \vdots & & & & \\ B_{N-m_A+2,1} & & B_{N-m_A+2,N-m_A+1} & B_{N-m_A+2,2} & \cdots & B_{N-m_A+2,N-m_A+2} & \cdots & B_{N-m_A+2,N} \\ \vdots & & \vdots & \vdots & & \vdots & & \vdots \\ B_{N1} & \cdots & B_{N,N-m_A+1} & B_{N2} & \cdots & B_{N,N-m_A+2} & \cdots & B_{NN} \end{pmatrix} \begin{pmatrix} i_1^{(1)} \\ i_1^{(2)} \\ \vdots \\ i_1^{(A)} \\ \hline i_2^{(1)} \\ \vdots \\ i_{m_1}^{(1)} \\ \vdots \\ i_2^{(A)} \\ \vdots \\ i_{m_A}^{(A)} \end{pmatrix} \tag{23}$$

$$\begin{pmatrix} C_{11} & C_{12} \\ \hline C_{21} & C_{22} \end{pmatrix} \begin{pmatrix} V_1 \\ \hline V_2 \end{pmatrix} = \begin{pmatrix} D_{11} & D_{12} \\ \hline D_{21} & D_{22} \end{pmatrix} \begin{pmatrix} I_1 \\ \hline I_2 \end{pmatrix} \tag{24}$$

$$C_{11} = \begin{bmatrix} A_{11}^{(1)} & & 0 \\ & A_{11}^{(2)} & \\ & \ddots & \\ 0 & & A_{11}^{(A)} \end{bmatrix} \quad C_{12} = \begin{bmatrix} A_{12}^{(1)} \cdots A_{1m_1}^{(1)} & \cdots & 0 \\ & A_{12}^{(2)} \cdots A_{1m_2}^{(2)} & \\ 0 & \cdots & A_{12}^{(A)} \cdots A_{1m_A}^{(A)} \end{bmatrix}$$

$$C_{21} = \begin{bmatrix} A_{21}^{(1)} & 0 \cdots & \\ A_{m_1 1}^{(1)} & 0 \cdots & \\ 0 \quad A_{21}^{(2)} & 0 \cdots & \\ 0 \quad A_{m_2 1}^{(2)} & 0 \cdots & \\ 0 \cdots & 0 & A_{21}^{(A)} \\ 0 \cdots & 0 & A_{m_A 1}^{(A)} \end{bmatrix} \quad C_{22} = \begin{bmatrix} A_{22}^{(1)} \cdots A_{2m}^{(1)} & & 0 \cdots 0 \\ A_{m_1 2}^{(1)} \cdots A_{m_1 m_1}^{(1)} & A_{22}^{(2)} \cdots A_{2m_2}^{(2)} & \\ 0 \cdots & A_{m_2 2}^{(2)} \cdots A_{m_2 m_2}^{(2)} & \cdots 0 \\ & & \\ 0 \cdots & & A_{22}^{(A)} \cdots A_{2m_A}^{(A)} \\ 0 \cdots & & A_{m_A 2}^{(A)} \cdots A_{m_A m_A}^{(A)} \end{bmatrix}$$

$$D_{11} = \begin{bmatrix} B_{11} & B_{1,m_1+1} & B_{1,N-m_A+1} \\ & & \\ B_{N-m_A+1,1} & \cdots & B_{N-m_A+1,N-m_A+1} \end{bmatrix}$$

$$D_{21} = \begin{pmatrix} B_{21} & B_{2,m_1+1} & \cdots & B_{2,N-m_A+1} \\ \vdots & & & \vdots \\ B_{m_1 1} & & & B_{m_1,N-m_A+1} \\ \vdots & & & \vdots \\ B_{N-m_A+2,1} & & & B_{N-m_A+2,N-m_A+1} \\ \vdots & & & \vdots \\ B_{N1} & & & B_{N,N-m_A+1} \end{pmatrix}$$

$$D_{12} = \begin{pmatrix} B_{12} & \cdots & B_{1m_1} & \cdots & B_{1,N-m_A+2} & \cdots & B_{1N} \\ \vdots & & & & & & \\ B_{N-m_A+1,2} & \cdots & B_{N-m_A+1,m_1} & \cdots & & & B_{N-m_A+1,N} \end{pmatrix}$$

$$D_{22} = \begin{pmatrix} B_{22} & \cdots & B_{2m_1} & \cdots & & B_{2,N-m_A+2} & \cdots & B_{2N} \\ \vdots & & \vdots & & & & & \\ B_{m_1 2} & \cdots & B_{m_1 m_1} & \cdots & & & & \\ \vdots & & \vdots & & & & & \\ B_{N-m_A+2,2} & \cdots & B_{N-m_A+2,m_1} & \cdots & B_{N-m_A+2,N-m_A+2} & & B_{N-m_A+2,N} \\ \vdots & & \vdots & & \vdots & & \vdots & \\ B_{N2} & \cdots & B_{Nm_1} & \cdots & B_{N,N-m_A+2} & \cdots & B_{NN} \end{pmatrix}$$

$$V_1 = \begin{pmatrix} v_1^{(1)} \\ v_1^{(2)} \\ \vdots \\ v_1^{(A)} \end{pmatrix} \qquad V_2 = \begin{pmatrix} v_2^{(1)} \\ \vdots \\ v_{m_1}^{(1)} \\ \vdots \\ v_2^{(A)} \\ \vdots \\ v_{m_A}^{(A)} \end{pmatrix}$$

$$I_1 = \begin{pmatrix} i_1^{(1)} \\ i_1^{(2)} \\ \vdots \\ i_1^{(A)} \end{pmatrix} \qquad I_2 = \begin{pmatrix} i_2^{(1)} \\ \vdots \\ i_{m_1}^{(1)} \\ \vdots \\ i_2^{(A)} \\ \vdots \\ i_{m_A}^{(A)} \end{pmatrix}$$

An important property of waveguide modes is the existence of a characteristic wave impedance. From the field theory point of view, each possible solution to the wave equation is called a mode. A TEM wave is called a transmission-line mode, and all other waves are called higher-order modes.

When assuming that the stripline is straight with sufficient length, only the TEM mode can propagate in the uniform stripline, and higher-order modes which exist at the port i are considered to be loaded by the reactive characteristic impedance matrix $[\mathbf{Z}_L^{(i)}]_{(m_i-1)x(m_i-1)}$.

$$[v_L^{(i)}]_{(m_i-1)x1} = [\mathbf{Z}_L^{(i)}]_{(m_i-1)x(m_i-1)} [i_L^{(i)}]_{(m_i-1)x1} \tag{25}$$

$$L = 2,3,.....,m_A$$

$$i = 1,2,.....,A$$

$$[\mathbf{Z}_L^{(i)}]_{pq} = -j\mathbf{Z}_c\{((L-1)\lambda / 2W_e\sqrt{\varepsilon_{re}})^2 - 1\}^{-1/2} \quad (p = q) \tag{26}$$

$$= 0 \tag{27}$$

$$p, q = 1,2,3,.....,m_i - 1 \qquad i = 1,2,.....,A$$

$$\mathbf{Z}_c = \frac{120\pi d}{W_e\sqrt{\varepsilon_{re}}} \tag{28}$$

d : the thickness of the substructure

W_e: the effective width of the stripline

ε_{re} : the effective relative dielectric constant

$$Z_L = \begin{pmatrix} [\,\mathbf{z}_L^{(1)}\,] & \cdots\cdots & 0 \\ \vdots & [\,\mathbf{z}_L^{(2)}\,] & \vdots \\ 0 & \cdots\cdots & [\,\mathbf{z}_L^{(A)}\,] \end{pmatrix} \qquad (29)$$

(N-A)x(N-A)

$$N = m_1 + m_2 + \cdots\cdots + m_A \qquad (30)$$

Then, we can find the relative equation for the higher order modes at each port.

$$V_2 = Z_L I_2 \qquad (31)$$

Based on analysis using contour-integral method, $[Z]_{AxA}$ (shown as Eq.44) the fundmental modes of the network at port 1,2,....,A can be extracted from TEM modes and loaded by the characteristic impedances of the higher order modes. $[Z]_{AxA}$ can be transformed into the scattering matrix (shown as Eq.46) directly as follows .

$$C_{11}V_1 + C_{12}V_2 = D_{11}I_1 + D_{12}I_2 \qquad (32)$$

$$C_{21}V_1 + C_{22}V_2 = D_{21}I_1 + D_{22}I_2 \qquad (33)$$

$$V_2 = Z_L I_2 \qquad (34)$$

$$C_{11}V_1 + C_{12}Z_L I_2 = D_{11}I_1 + D_{12}I_2 \qquad (35)$$

$$C_{21}V_1 + C_{22}Z_L I_2 = D_{21}I_1 + D_{22}I_2 \tag{36}$$

$$C_{11}V_1 = D_{11}I_1 + (D_{12} - C_{12}Z_L)\, I_2 \tag{37}$$

$$C_{21}V_1 = D_{21}I_1 + (D_{22} - C_{22}Z_L)\, I_2 \tag{38}$$

$$C_{11}V_1 + (C_{12} - D_{12}Z_L^{-1})\, V_2 = D_{11}I_1 \tag{39}$$

$$C_{21}V_1 + (C_{22} - D_{22}Z_L^{-1})\, V_2 = D_{21}I_1 \tag{40}$$

from (39),(40)

$$(C_{22} - D_{22}Z_L^{-1})\, V_2 = -C_{21}V_1 + D_{21}I_1 \tag{41}$$

$$V_2 = -(C_{22} - D_{22}Z_L^{-1})^{-1} C_{21}V_1 + (C_{22} - D_{22}Z_L^{-1})^{-1} D_{21}I_1 \tag{42}$$

substitute (42) into (39)

$$[C_{11} - (C_{12} - D_{12}Z_L^{-1})(C_{22} - D_{22}Z_L^{-1})^{-1} C_{21}]\, V_1 =$$

$$[D_{11} - (C_{12} - D_{12}Z_L^{-1})(C_{22} - D_{22}Z_L^{-1})^{-1} D_{21}]\, I_1 \tag{43}$$

$$[Z]_{AxA} = [\, C_{11} - (\, C_{12} - D_{12}Z_L^{-1})(\, C_{22} - D_{22}Z_L^{-1})^{-1} C_{21}]^{-1}$$

$$[\, D_{11} - (\, C_{12} - D_{12}Z_L^{-1})(\, C_{22} - D_{22}Z_L^{-1})^{-1} D_{21}] \qquad (44)$$

$$[Z]_{AxA} = \begin{pmatrix} Z_{11} & \cdots & Z_{1A} \\ Z_{21} & & \vdots \\ \vdots & & \\ Z_{A1} & \cdots & Z_{AA} \end{pmatrix} \qquad (45)$$

$$[S] = [\sqrt{Y_0}\,]\,([Z] - [Z_0])\,([Z] + [Z_0])^{-1}[\sqrt{Z_0}\,] \qquad (46)$$

$$[Z_0] = \begin{pmatrix} Z_{01} & \cdots & 0 \\ \vdots & Z_{02} & \vdots \\ & \ddots & \\ 0 & \cdots & Z_{0A} \end{pmatrix} \qquad (47)$$

$$[Y_0] = 1/[Z_0] \qquad (48)$$

Numerical results

1. Right-angled bend with and without a miter cut : (Fig.1 a.b)

Shown in Fig.6 is the variation in the reflection coefficient $|S_{11}|$ for chamfered and unchamfered right-angle bends. The results are compared with Gupta's results [9]. In order to reduce the effect of the discontinuity reactances, an isosceles triangle part must be removed. The size of the triangle removed has been optimized, to minimize the reflection coefficient . Figure 7 shows that when a measured cut ratio c/w is equal to about 0.8, the V.S.W.R. is minimized. Kaneko has the same conclusions[7].

2. T-junction without a miter cut : (Fig. 2a)

Results for frequency dependent scattering matrix coefficients for a T-junction ($\varepsilon_r = 9.7$, d = 0.0635 cm, w_2=0.056 cm) are shown in Fig.8. It notes that $|S_{22}|$, as shown in Fig 8a, the power reflected by the T-junction discontinuities increases with frequency in the range $0 < f < f_{c1}$, where f_{c1} is the cut-off frequency of the first higher order mode. Correspondingly, the power transmitted from port 1 to port 2 decreases with frequency greater than f_{c1}. The power of a port is transmitted by the first higher order mode, so that the transmission coefficient $|S_{12}|$ is always smaller than that for f = 0 (shown in Fig.8b).

Fig.8c indicates that, if the TEM mode is incident at port 1, the reflected power decreases with increasing frequency, and another power transmitted to port 3 behaves in an opposite sense to $|S_{12}|$. Also plotted in Fig.8 are the numerical results reported in [8].

3. T - junction with a V - shaped miter cut : (Fig. 2b)

This section considers a T-junction with an isosceles triangle with angle $\theta = 45^{o}$ removed; the side of the triangle removed is equal to c (cut depth). For a cut ratio c/w2 = 0.4035..., the scattering coefficients are plotted in Fig.9. The reported data [9] is also plotted in fig.9. When the frequency increases, the variation of the magnitude of reflected coefficient $|S_{11}|$ keeps almost constant and is between a range of 0.41 to 0.45. The predicted value of $|S_{22}|$ is greater than the published value by 2.5 percent.

For different cut ratios, Fig.10 shows clearly that by removing an isosceles triangle from a T - junction with $\theta = 45\backslash s(0,)$ and c/w2 = 0.8, the effects of $|S_{11}|$ are minimized at the higher frequency band . This phenomenon is similar to the case of right-angled microstrip bend with a miter cut ratio 0.8. By considering a plane of symmetry located at half the width of port 2, the T-junction can be compared with a right-angled bend on just one side of the symmetrical plane. The reflection coefficient $|S_{11}|$ is equal to $|S_{33}|$ of the corresponding side of the bend. Thus, if only $|S_{11}|$ or $|S_{33}|$ is to be optimized, then only a right-angled bend with one half of the width of port 2 need to be considered.

In the boundary - integral method, the circuit periphery is divided into N sections , the value of N determines the size of NxN impedance matrix [Z] . The greater N is , the more precise the result will be. The error decreases from 8 to 2.5 percent with N increased from 80 to 300 (Fig.11). Also, for the purpose of saving computer time, the problem of properly selecting the location of each scattering point become more important when the effective width of each port is not the same.

Conclusion

Computer-aided-design is a very powerful tool in the circuit design of MIC and MMIC. A great savings of time and money can be resulted if a design is verified before it is fabricated. The work described in this paper showed how the boundary-integral method can be used to solve planar microstrip circuits. The results discussed here are in excellent agreement with other methods for the right-angled bend and T-junction. Future studies will concentrate on developing this method for more complicated microstrip discontinuities.

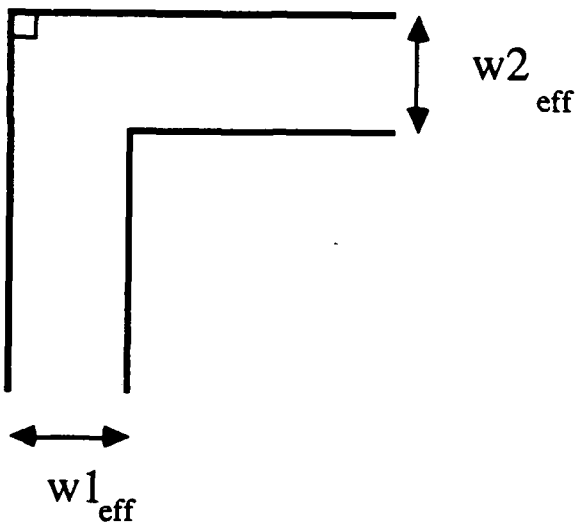

Fig. 1a

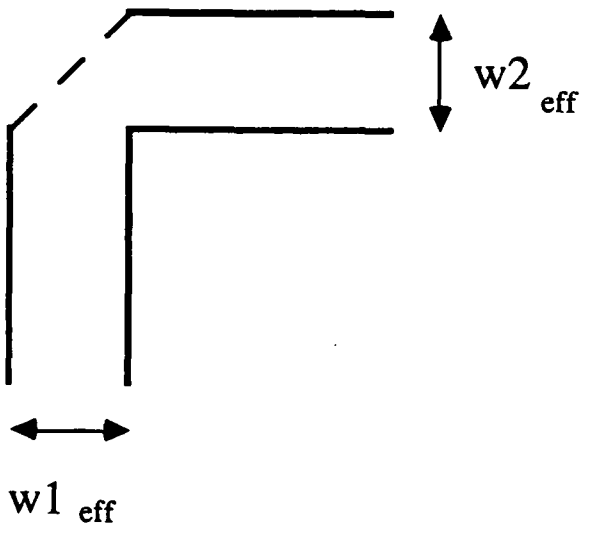

Fig. 1b

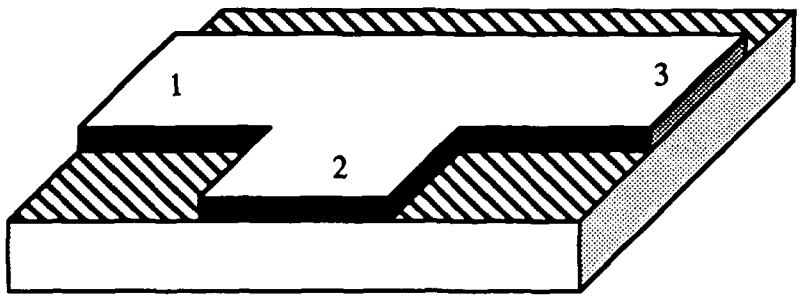

Microstrip T- junction structure

Fig. 2a

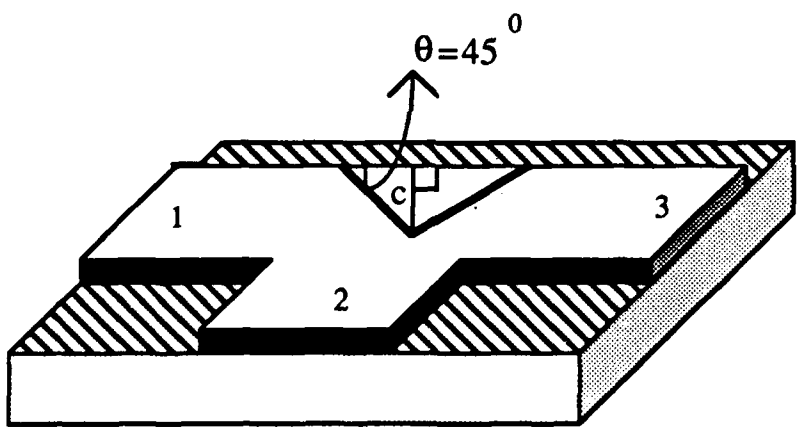

T-junction microstrip with a V-shape cut

Fig . 2b

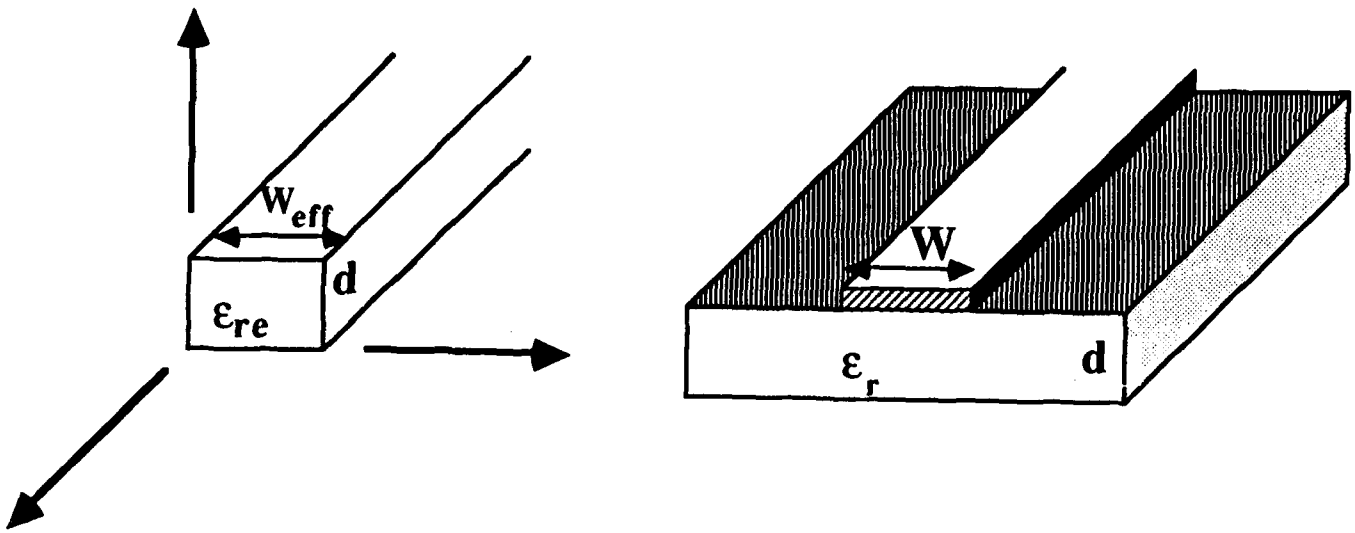

Fig. 3

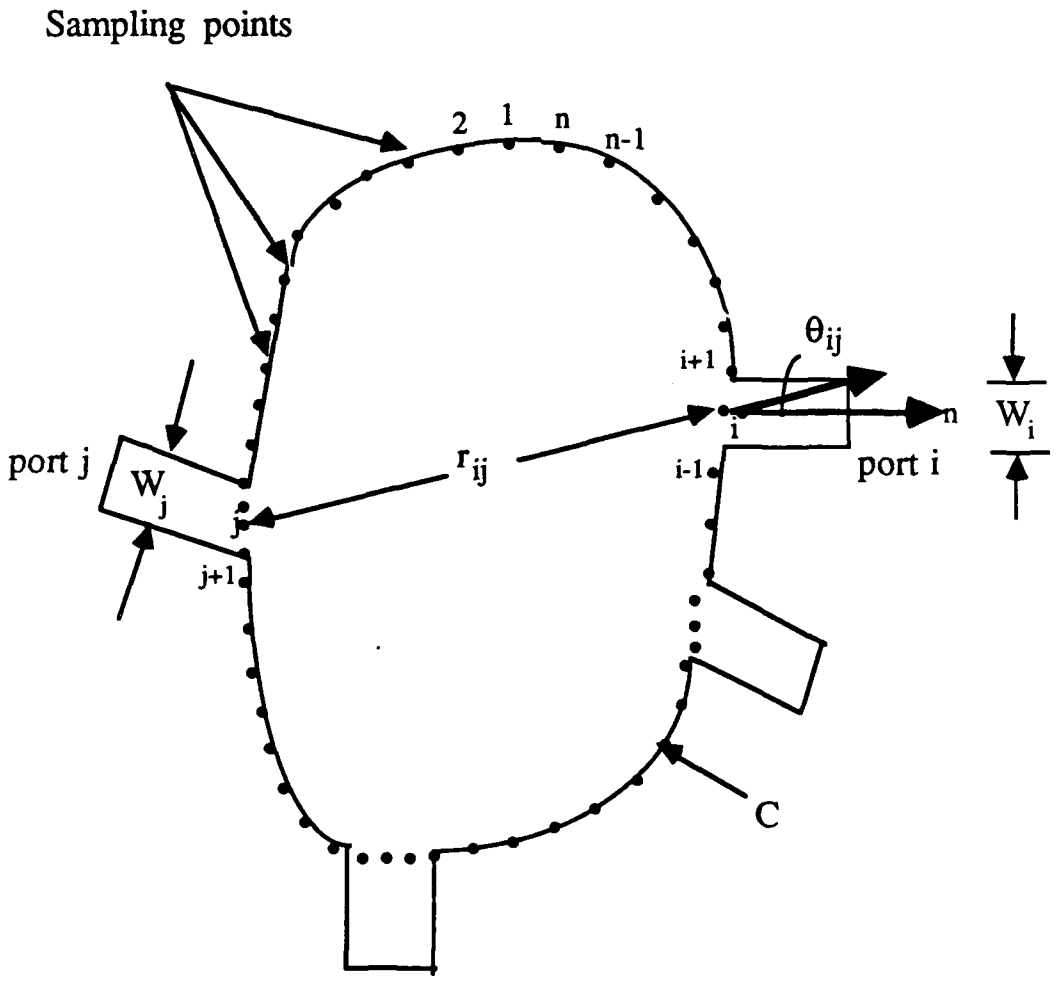

Fig. 4

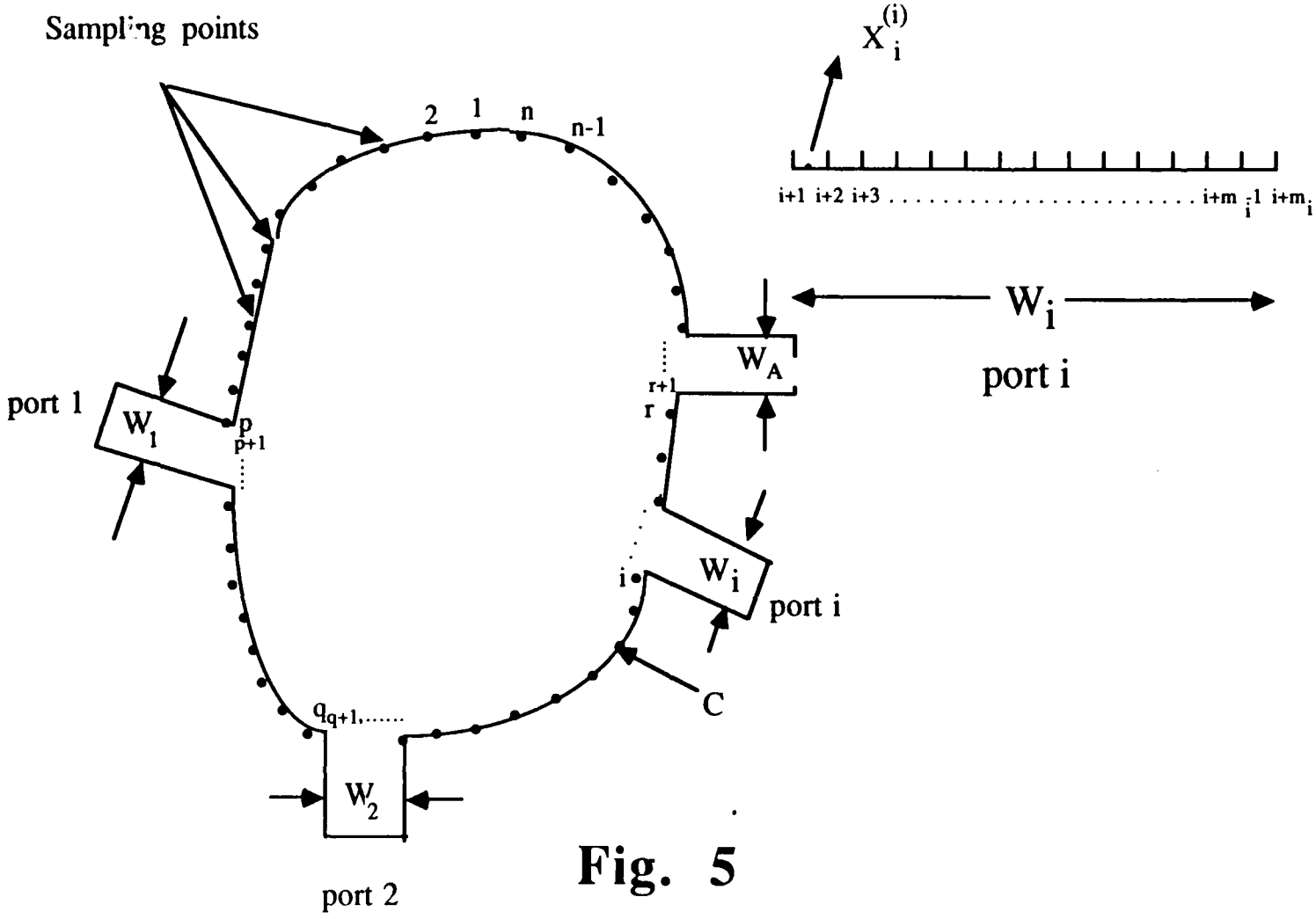
Sampling points
$X_i^{(i)}$
2
1
n
n-1
i+1 i+2 i+3 . . . . . i+m_i-1 i+m_i
W_i
port i
W_A
r+1
r
port 1
W_1
p
p+1
i
W_i
port i
C
q_{q+1},.....
W_2
port 2

Fig. 5

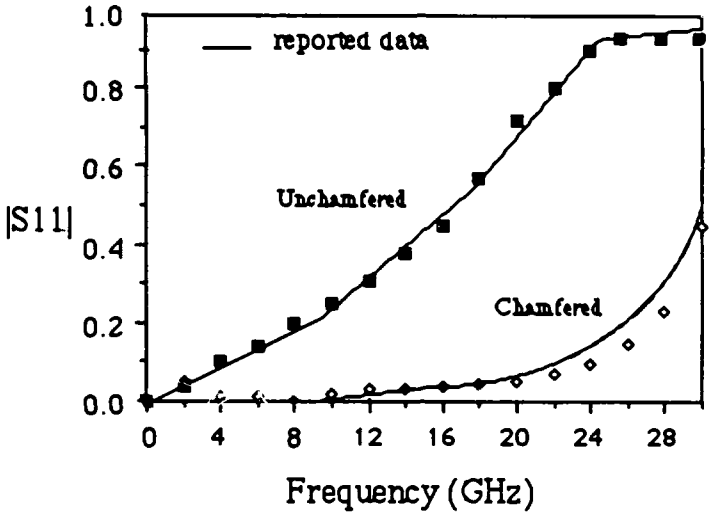

Fig. 6

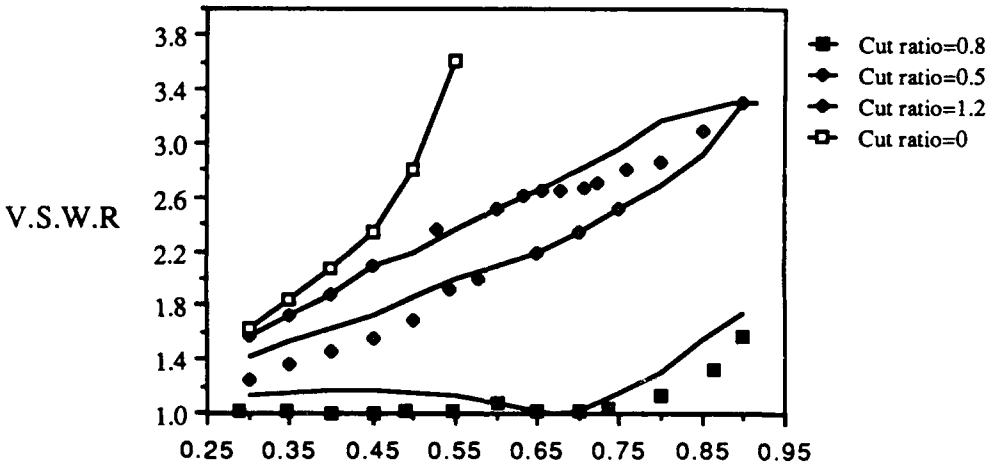

$W1_{eff}=W2_{eff}=0.056cm, d=0.0635cm, \varepsilon_r=9.7$

Fig. 7

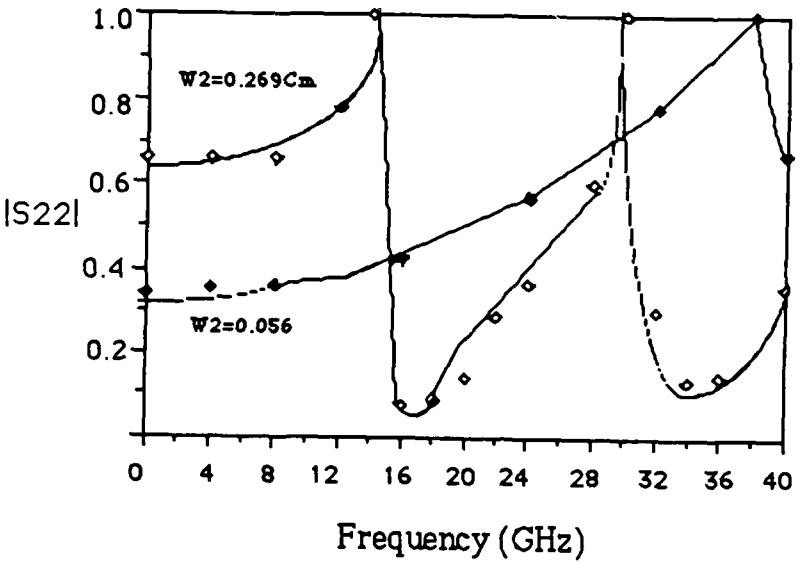
1.0
0.8
0.6
0.4
0.2
|S22|
W2=0.269Cm
W2=0.056
0
4
8
12
16
20
24
28
32
36
40
Frequency (GHz)
reported data

Fig. 8a

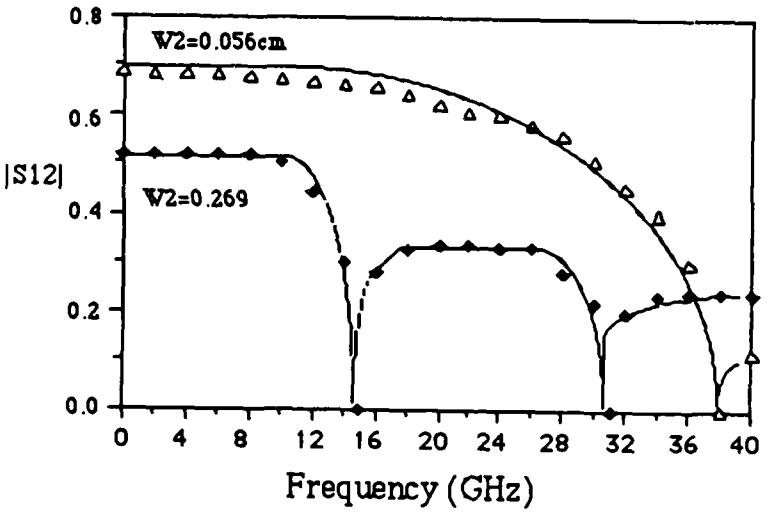
0.8
0.6
0.4
0.2
0.0
|S12|
W2=0.056cm
W2=0.269
0
4
8
12
16
20
24
28
32
36
40
Frequency (GHz)
reported data

Fig. 8b

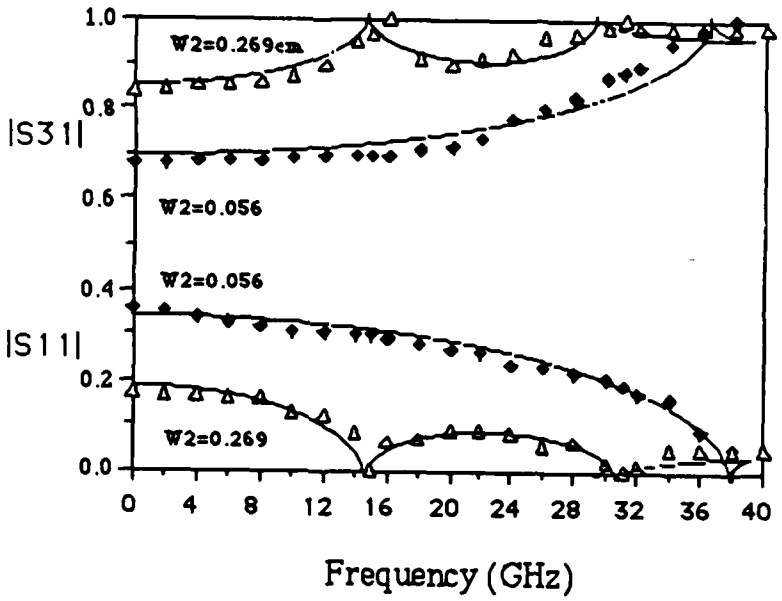
1.0
0.8
0.6
0.4
0.2
0.0
|S31|
|S11|
W2=0.269cm
W2=0.056
W2=0.056
W2=0.269
0
4
8
12
16
20
24
28
32
36
40
Frequency (GHz)
reported data

Fig. 8c

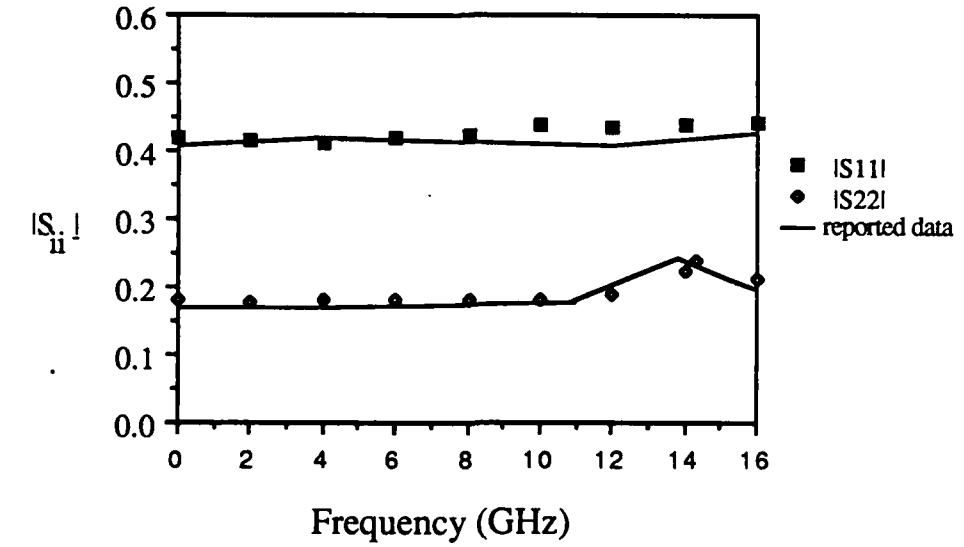
0.6
0.5
0.4
0.3
0.2
0.1
0.0
$|S_{ii}|$
0
2
4
6
8
10
12
14
16
|S11|
|S22|
reported data
Frequency (GHz)

Fig. 9

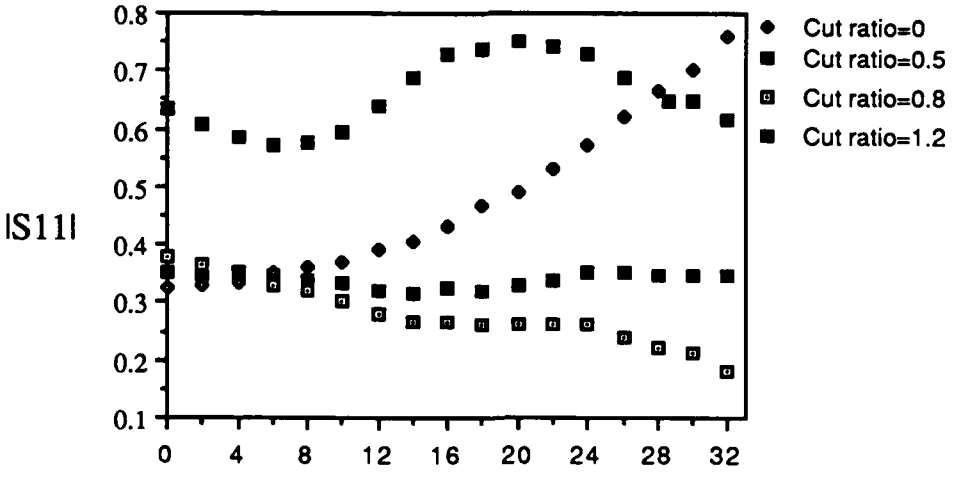
0.8
0.7
0.6
0.5
0.4
0.3
0.2
0.1
|S11|
0
4
8
12
16
20
24
28
32
Cut ratio=0
Cut ratio=0.5
Cut ratio=0.8
Cut ratio=1.2
Frequency (GHz)

Fig. 10

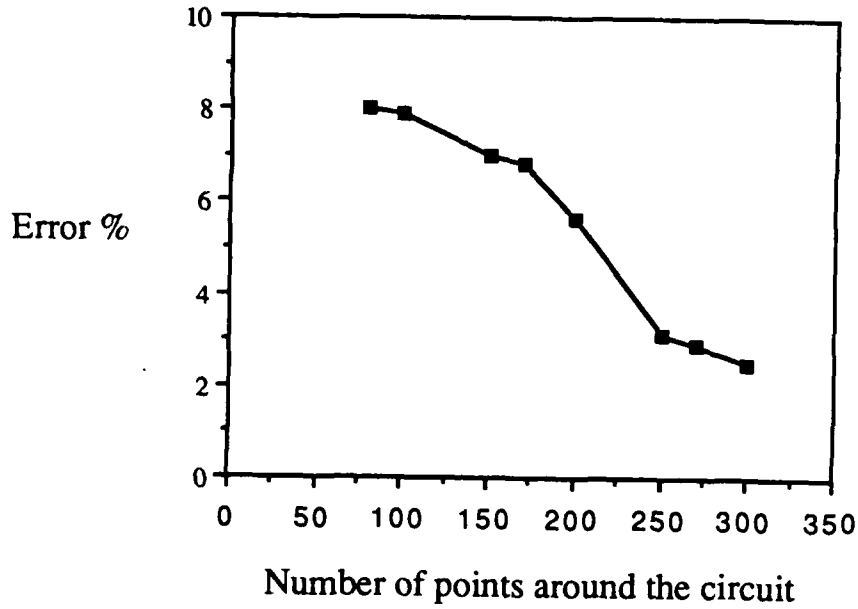
Error %
10
8
6
4
2
0
0
50
100
150
200
250
300
350
Number of points around the circuit

Fig. 11

Reference

[1] R. Chadha and K. C. Gupta, " Segmentation method using impedance matrices for the analysis of planar microwave circuits," IEEE Trans. Microwave Theory Tech., vol. MTT-29, pp.71-74, Jan. 1981.

[2] P. C. Sharma and K. C. Gupta, "Desegmentation method for analysis of two-dimension microwave circuits," IEEE Trans. Microwave Theory Tech., vol. MTT-29, pp.1094-1098, Oct. 1981.

[3] K. C. Gupta, R. Chadha and P. C. Sharma, " Two-dimensional analysis for stripline/microstrip circuits," IEEE MTT-S Int. Symp. Dig., pp. 504-506, June 1981.

[4] R. Chadha and K. C. Gupta, " Green's functions for triangular segments in planar microwave circuits," IEEE Trans. Microwave Theory Tech., vol. MTT-28, pp.1139-1143, Oct. 1981 .

[5] Takanori Okoshi, Planar circuits for microwaves and lightwaves, New York: Springer-Verlag, Chapter 3., 1985.

[6] J. A. Stratton, Electromagnetic Theory, New York: McGraw-Hill, 1941, p.460.

[7] Hitoshi Kaneko, Hsu Jui-Pang, "Analysis of rightangle corner by normal mode method," Electronics Communication Association of Japan, MW-76-13, 1983.

[8] K. C. Gupta, Microstrip lines and slotlines, Dedham: Artech, pp.172, 1979.

[9] Rakesh Chadha and K.C. Gupta, "Compensation of discontinuities in planar transmission lines," IEEE Trans. Microwave Theory Tech.,vol. MTT-30, pp.2153-2155, Dec.1982.

VITA

Sanchi Sandy Chang [redacted] After completing her work at The Taipei First Girls' Senior High School, Taipei, Taiwan, R.O.C., in 1983, she entered Tam Kang University, Taipei, Taiwan. She received the degree of Bachelor of Science from Tam Kang University in June, 1987. In September, 1987, she entered The Graduate School of The University of Texas.

[redacted]